

USING MILLIMETER VLBI TO CONSTRAIN RIAF MODELS OF SAGITTARIUS A*

VINCENT L. FISH¹, AVERY E. BRODERICK², SHEPERD S. DOELEMEN¹, & ABRAHAM LOEB³

May 29, 2019

ABSTRACT

The recent detection of Sagittarius A* at $\lambda = 1.3$ mm on a baseline from Hawaii to Arizona demonstrates that millimeter wavelength very long baseline interferometry (VLBI) can now spatially resolve emission from the innermost accretion flow of the Galactic center region. Here, we investigate the ability of future millimeter VLBI arrays to constrain the spin and inclination of the putative black hole and the orientation of the accretion disk major axis within the context of radiatively inefficient accretion flow (RIAF) models. We examine the range of baseline visibility and closure amplitudes predicted by RIAF models to identify critical telescopes for determining the parameters of the Sgr A* black hole and accretion disk system. We find that baseline lengths near $3 G\lambda$ have the greatest power to distinguish amongst RIAF model parameters, and that it will be important to include either the Large Millimeter Telescope or a Chilean telescope in future VLBI arrays. Many RIAF models predict detectable fluxes on baselines between the continental United States and even a single 12 m-class dish in Chile. The extra information provided from closure amplitudes by a four-antenna array enhances the ability of VLBI to discriminate amongst models.

Subject headings: black hole physics — accretion, accretion disks — submillimeter — Galaxy: center — techniques: interferometric

1. INTRODUCTION

The Galactic center radio source Sagittarius A* is believed to be associated with a black hole with a mass of approximately $4 \times 10^6 M_\odot$ at a distance of about 8 kpc (Schödel et al. 2003; Ghez et al. 2008). The event horizon of Sgr A* has the largest apparent angular size of all known black holes as viewed from Earth. High angular resolution is critical to understanding Sgr A* because the size scales are so small: for instance, the apparent lensed horizon size is $55 \mu\text{as}$. The quest for angular resolution has driven observers toward very long baseline interferometry (VLBI) at millimeter wavelengths. Most recently, Doeleman et al. (2008a) detected Sgr A* at 230 GHz ($\lambda = 1.3$ mm) on baselines between the James Clerk Maxwell Telescope (JCMT) in Hawaii and the Submillimeter Telescope Observatory (SMTO) in Arizona, as well as between the SMTO and a Combined Array for Research in Millimeter-wave Astronomy (CARMA) telescope in California. The former is the longest baseline ($3.5 G\lambda$, fringe spacing $\sim 60 \mu\text{as}$) on which Sgr A* has ever been detected.

In the absence of a full three-dimensional general relativistic magnetohydrodynamic simulation of the accretion flow of Sgr A*, many simplified physical models of the emission region have been proposed. For instance, there is still a vigorous debate over whether the emission is produced predominantly by a hot accretion disk or from an energetic outflow. The constraints provided by the multiwavelength spectrum, variability, and polarization of Sgr A* do not yet conclusively establish the nature of the emission region. The predicted observable signatures will depend on key physical parameters such as the accretion rate, black hole spin, and the orientation of the disk or jet, which are not known a priori. Millimeter VLBI may be able to discriminate amongst models of the

emission region, but it is important to understand how they depend upon the parameters of the Sgr A* system. Conversely, if the context of the emission can be conclusively established, millimeter VLBI has great potential to extract these parameters.

In a related work, Broderick et al. (2008) examine the ability of the Doeleman et al. (2008a) VLBI detections to discriminate amongst various radiatively inefficient accretion flow (RIAF) models parameterized by black hole spin, viewing angle, and disk orientation. A key finding is that the detected flux on the JCMT-SMTO baseline argues against orientations in which the assumed accretion disk is close to face on. However, the RIAF parameters are strongly coupled, and there are not yet enough millimeter VLBI measurements to make strong statements about the black hole spin, for instance. In this work, we explore the question of which millimeter VLBI observations are likely to have the greatest impact for distinguishing between RIAF models and are therefore most likely to determine the physical parameters of the black-hole/accretion-disk system.

2. DISK MODELS AND TELESCOPES

Details of quiescent RIAF disk modelling can be found in Broderick & Loeb (2005, 2006) and Doeleman et al. (2008b). We consider an ensemble of such models, each with a total flux density of 2.4 Jy at $\lambda = 1.3$ mm, in line with the integrated flux density measured by Doeleman et al. (2008a). Models are parameterized by black hole spin (a), inclination ($\theta = 0^\circ$ for a face-on disk), and orientation of the disk major axis on the plane of the sky (ξ , measured counterclockwise from east). Models are produced at spins from $a = 0.0$ to 0.9 in increments of 0.1 , as well as at 0.99 and 0.998 . The ensemble includes models at $\theta = 1^\circ$ and then at $\theta = 10^\circ$ to 90° in 10° increments. This particular model set is described in greater detail in Broderick et al. (2008). We consider models with $0^\circ \leq \xi < 180^\circ$ with an increment of $\Delta\xi = 5^\circ$ (in §3.1) or 30° (in §§3.2 and 3.3). Visibility amplitudes are symmetric under 180° rotation for any real intensity distribution.

We consider seven potential stations for millimeter VLBI:

¹ Massachusetts Institute of Technology, Haystack Observatory, Route 40, Westford, MA 01886; vfish@haystack.mit.edu.

² Canadian Institute for Theoretical Astrophysics, University of Toronto, 60 St. George St., Toronto, ON, M5S 3H8 Canada.

³ Institute for Theory and Computation, Harvard University, Center for Astrophysics, 60 Garden St., Cambridge, MA 02138.

Hawaii, consisting of one or more of the JCMT, Submillimeter Array (SMA), and Caltech Submillimeter Observatory (CSO) possibly phased together into a single aperture; the SMTO on Mount Graham, Arizona; CARMA telescopes in California, either individually or phased together; the Large Millimeter Telescope (LMT) on Sierra Negra, Mexico; a Chilean station consisting of either the Atacama Submillimeter Telescope Experiment (ASTE), Atacama Pathfinder Array (APEX), or a phased array of Atacama Large Millimeter Array (ALMA) dishes; the Institut de radioastronomie millimétrique (IRAM) 30-m dish on Pico Veleta (PV), Spain; and the IRAM Plateau de Bure (PdB) Interferometer, phased together as a single aperture. Assumed telescope capabilities and sensitivities are detailed in Doeleman et al. (2008b).

3. BLACK HOLE PARAMETER ESTIMATION

3.1. Favored Regions of the (u, v) Plane

For the purpose of distinguishing different RIAF models, it is most desirable to obtain observations of Sgr A* on baselines at points at which the RIAF visibilities are most disparate. We compute RIAF model visibilities

$$V(u, v) = \iint dx dy I(x, y) e^{-2\pi i(xu + yv)/\lambda},$$

where $I(x, y)$ is the model intensity distribution with x and y are aligned east and north, respectively. We characterize the variation in RIAF model visibilities via the standard deviation $\sigma(u, v)$ amongst all RIAF models. While we initially ignore the effects of interstellar scattering, it can be included by multiplying the visibilities by a unit-normalized elliptical Gaussian centered at the origin (half width at half maximum of $7.0 \times 3.8 \text{ G}\lambda$, position angle 170° east of north, based on Bower et al. 2006).

Figure 1 shows the scatter in predicted model visibilities, $\sigma(u, v)$. The peak standard deviation occurs at a baseline length of approximately $3 \text{ G}\lambda$ at $\lambda = 1.3 \text{ mm}$ ($\sim 4000 \text{ km}$) aligned with the accretion disk major axis. Since the disk orientation (ξ) is not known a priori, the optimal baseline orientation is unknown.

Not all RIAF models are equally likely, however. The Doeleman et al. (2008a) detections of correlated flux densities on the JCMT-SMTO and SMTO-CARMA baselines as well as with the CARMA interferometer place constraints on RIAF models. Following the approach of Broderick et al. (2008), we compute the probability $p(a, \theta, \xi)$ for every RIAF model based on the Doeleman et al. (2008a) detections, including a $\sin \theta$ prior on the inclination. Restricting the ensemble of models to those with $p \geq 0.01 p_{\text{max}}$ (or approximately one-quarter of the total set of models), we can obtain the scatter in the predicted correlated flux densities of the most *probable* RIAF models, $\sigma_p(u, v)$ (Fig. 2). We find that the largest scatter in models still occurs at baseline lengths near $3 \text{ G}\lambda$, but at orientations substantially different from that of the JCMT-SMTO detection (labelled “HS” in Fig. 2), which has already placed a stringent constraint on RIAF models in its region of (u, v) space.

3.2. Implications for Specific Baselines

Figure 3 shows predicted correlated flux densities on potential millimeter VLBI baselines for the probable RIAF models. Each pair of telescopes produces visibility measurements along a range of projected baseline lengths due to the Earth’s rotation. These correlated flux densities have been corrected for interstellar scattering.

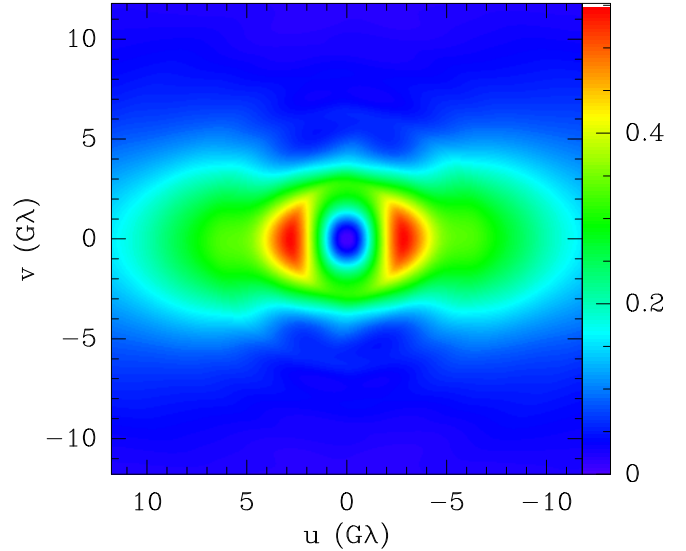


FIG. 1.— Map of standard deviation of predicted RIAF model visibilities ($\sigma(u, v)$) at $\lambda = 1.3 \text{ mm}$ holding $\xi = 0^\circ$ constant. Units are in Jy. The largest spread in predicted model quantities occurs when the projected baseline is aligned with the disk major axis. Rotating the image on the plane of the sky produces a rotation of the visibility amplitudes in the (u, v) plane.

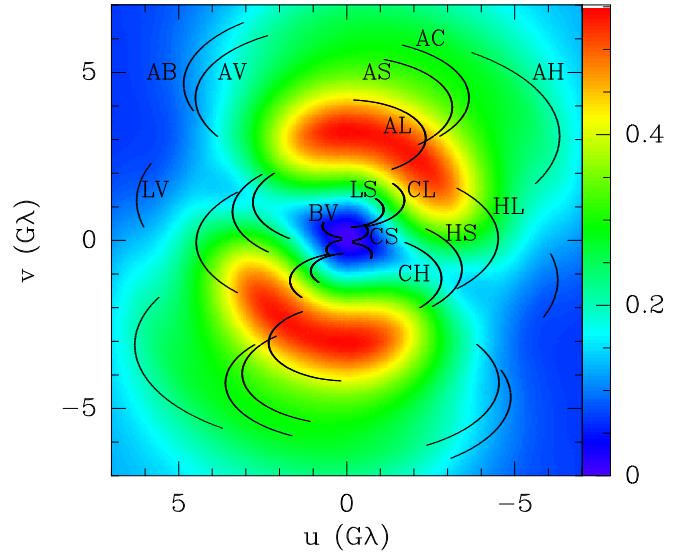


FIG. 2.— Plot of the standard deviation $\sigma_p(u, v)$ restricted to the most probable RIAF models (see §3.1) on the inner part of the (u, v) plane at $\lambda = 1.3 \text{ mm}$. Units are in Jy. Potential (u, v) tracks due to Earth rotation are superposed, with letters indicating antennas. A: APEX/ASTE/ALMA, B: PdB, C: CARMA, H: Hawaii (incl. JCMT), L: LMT, S: SMTO, V: PV

Detections have already been obtained on the Hawaii-SMTO and SMTO-CARMA baselines, although Sgr A* was not detected on the Hawaii-CARMA baseline (Doeleman et al. 2008a). It is likely that the next millimeter VLBI observations of Sgr A* will occur on an array containing these same three stations, although with the inclusion of a phased-array processor at Hawaii to sum the signals from the JCMT, CSO, and SMA. The increased sensitivity should allow Sgr A* to be detected on the Hawaii-SMTO baseline with a higher signal-to-noise ratio, tightening the constraints on RIAF models especially if Sgr A* can be detected on scans when it is low to the horizon from Arizona, where the range of predicted model flux densities is larger. The Hawaii-CARMA baseline will be more sensitive than the Hawaii-SMTO baseline once the planned array

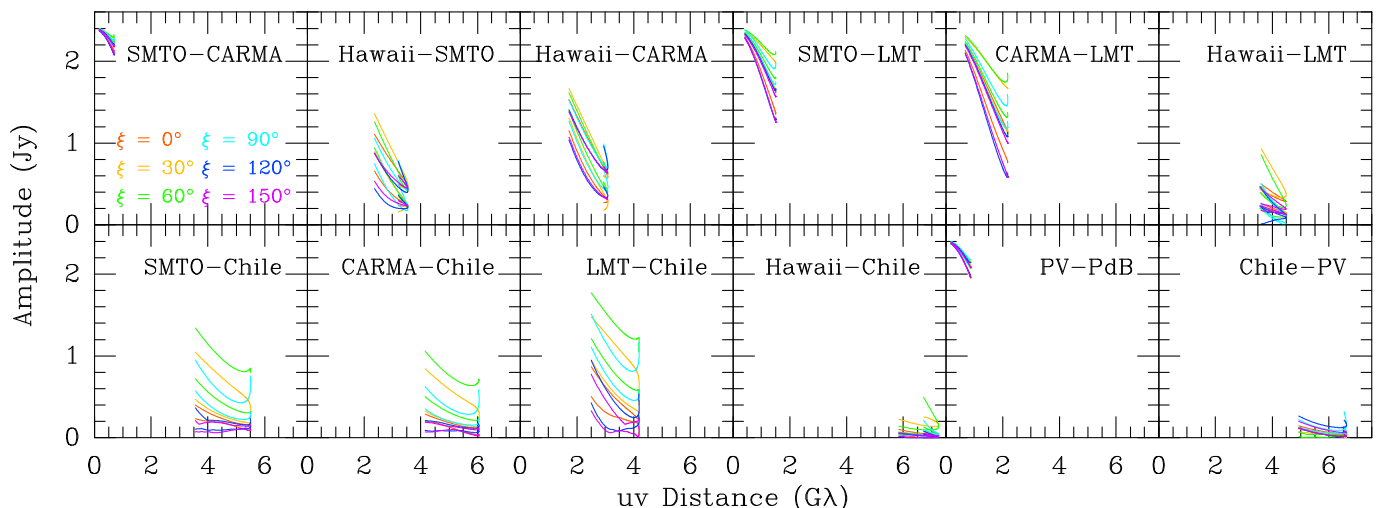


FIG. 3.— Predicted model fluxes on potential baselines. Each panel shows the predicted track of correlated flux density with $\sqrt{u^2 + v^2}$ (changing due to Earth rotation) for one baseline for all models ($\Delta\xi = 30^\circ$) for which $p > 0.01 p_{\max}$. Lines show the maximum and minimum predicted correlated flux density from the set of probable RIAF models with a given disk orientation, shown in color. The visibility amplitudes on many baselines are highly sensitive to ξ . LMT-Chile provides the greatest power in further constraining RIAF parameter space, followed by baselines from the continental U.S. to either the LMT or Chile.

phasing capability is added to CARMA, although the range in predicted model flux densities is somewhat smaller on Hawaii-CARMA. Because the predicted flux densities on the Hawaii-CARMA and Hawaii-SMT0 baselines are similar due to their location in approximately the same location of the (u, v) plane, strongly constraining key black hole and accretion disk parameters will necessitate obtaining flux density measurements on other baselines as well. However, measurements on the Hawaii-CARMA baseline may be important to establish the validity of RIAF models of Sgr A* in general and rule out simpler, less physically-motivated models, such as a Gaussian or a ring.

The optimal baseline for further constraining RIAF parameter space is LMT-Chile, which is in the preferred zone of baseline lengths and at a position angle nearly orthogonal to that of Hawaii-SMT0. Baselines from the continental United States to the LMT and Chile also show a large spread in predicted flux densities. Many of the models predict flux densities of well over 500 mJy (some even above 1 Jy) on the SMT0-Chile and CARMA-Chile baselines. These flux densities should be detectable even if a single ALMA dish is used for the Chilean station. Even a robust nondetection on these baselines would have great discriminatory power among the likely RIAF models.

Baseline correlated flux densities depend strongly on disk orientation. The scatter within the predicted correlated flux density for each baseline is much smaller when restricted to one value of ξ than when the entire model space ($\Delta\xi = 30^\circ$) is considered as a whole (Fig. 3). On most Western hemisphere baselines, predicted correlated flux densities are much higher near $\xi = 60^\circ$ than near $\xi = 150^\circ$.

The European telescopes are poorly placed for constraining RIAF models. The PV-PdB baseline has insufficient angular resolution, and baselines between Europe and the Americas resolve out most of the flux of Sgr A*. Nevertheless, it will be essential to obtain data on the long baselines to Europe as well as the Hawaii-Chile baseline eventually to verify the RIAF hypothesis as well as to detect (changing) small-scale inhomogeneities not modelled here. Longer term, the European telescopes will provide essential complementary (u, v) coverage for high-resolution millimeter imaging of Sgr A*.

3.3. Potential Complications

The flux density of 2.4 Jy at 230 GHz detected by Doeleman et al. (2008a) is low compared to measurements with the SMA (Marrone et al. 2007, 2008) and high compared to measurements with BIMA (Zhao et al. 2003; Bower et al. 2005) and a PV-PdB VLBI measurement at 215 GHz (Krichbaum et al. 1998). Sgr A* exhibits variability, although the consistent fluxes measured on two consecutive days by Doeleman et al. (2008a) suggest that Sgr A* was observed in its quiescent state. Since the variability mechanism is not understood, it remains unclear how variability in the total flux density of Sgr A* at millimeter wavelengths will affect the correlated flux densities measured on diverse VLBI baselines. Multiple epochs of observation will be essential to exploring the link between total flux variability and spatial structure around Sgr A*. It will also be important to obtain contemporaneous measurements of fluxes on a variety of baselines as well as a simultaneous “zero-spacing” flux density, preferably from a connected-element interferometer.

Variable and elevation-dependent antenna gains may limit the accuracy to which telescope flux scales can be derived, introducing systematic errors into calculations of correlated flux densities. These systematic errors may be difficult to characterize accurately and may limit the ability of baseline-based quantities to distinguish between RIAF models. Closure amplitudes are robust against station-based gain variations and will provide model constraints with significantly reduced systematic errors. If observations are taken with at least four telescopes, closure amplitudes can be constructed from ratios of baseline visibilities ($A_{abcd} = |V_{ab}| |V_{cd}| |V_{ac}|^{-1} |V_{bd}|^{-1}$, where subscripted letters identify telescopes).

RIAF models predict a wide range of closure amplitudes on quadrangles of four telescopes, as shown in Figure 4. While even a single measurement of a closure amplitude will be useful, multiple measurements of closure amplitudes on a quadrangle with time will have even greater power in further constraining RIAF parameter space, since different RIAF models can predict strongly differing closure amplitudes over a night of observations. As is the case for baseline visibilities, closure amplitudes are most highly sensitive to variations in ξ among the most probable models. From a closure amplitude perspec-

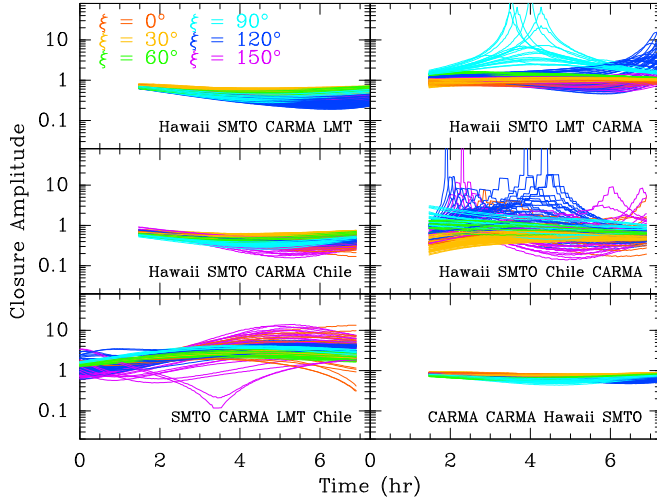


FIG. 4.— Predicted model closure amplitudes for all probable RIAF models over the time range for which Sgr A* is above 5° elevation at at least four of the five Western hemisphere stations. Colors are as in Figure 3. Small jumps in the Hawaii-SMTO-Chile-CARMA panel are artifacts in precision when the Hawaii-Chile baseline passes through a null. A single closure amplitude can also be formed by using two telescopes at the same site, such as CARMA. Closure amplitudes are highly sensitive to ξ and are robust against flux calibration errors.

tive, either Chile or the LMT would make an excellent fourth station in an observing array, although the low predicted correlated flux densities on the Hawaii-Chile baseline may make measurement of a second closure amplitude on an array consisting only of Hawaii, SMTO, CARMA, and Chile difficult without the use of phased-ALMA as the Chilean station.

An alternative observational strategy in the absence of a fourth telescope site would be to use two different telescopes at the same location, for instance at the CARMA site or in Hawaii. A single nontrivial closure amplitude can be formed from the resulting visibilities. The closure amplitude resulting from two CARMA antennas, the SMTO, and Hawaii has less power to differentiate among RIAF models than other four-antenna arrays (Fig. 4), but multiple detections over a single scan may still be useful. The redundant information provided by the double baselines between the CARMA site and another antenna will also aid in the detection of fringes and reduce the systematic uncertainty in correlated flux densities on the CARMA baselines. Given the nondetection of Sgr A* on the JCMT-CARMA baseline by Doeleman et al. (2008a), it is likely that this strategy would require the use of a phased-array processor at Hawaii.

4. CONCLUSIONS

The planned evolution of millimeter VLBI capability over the next few years will place strong constraints on RIAF models of Sgr A* emission. It is important to devise an observing strategy to test the RIAF hypothesis and extract information on the physical parameters of Sgr A* and its putative accretion disk. By identifying differences between RIAF models that are consistent with present VLBI observations, we identify five key points to guide future millimeter VLBI observations:

1. There is a preferred zone of baseline lengths near 3λ where there is enough angular resolution to distinguish between many of the RIAF models but not so much resolution that a large amount of flux is lost. The JCMT-SMTO detections are in this zone. The construction of a phased-array processor for the Hawaiian millimeter telescopes will allow for even tighter constraints to be placed on RIAF model parameters on the Hawaii-SMTO baseline as well as increase the chance of detecting Sgr A* on other baselines to Hawaii.

2. There is a strong correlation between fluxes on the Hawaii-SMTO and Hawaii-CARMA baselines, limiting the ability of the latter baseline to place extra constraints on RIAF parameters unless a phased-array processor is installed at CARMA, making Hawaii-CARMA a more sensitive baseline than Hawaii-SMTO. Nevertheless, the Hawaii-CARMA measurement will be important both for ruling out simpler models (e.g., a Gaussian or annulus) of the emission from Sgr A* that the present VLBI measurements cannot and for testing the RIAF hypothesis.

3. The single baseline with the greatest power to discriminate amongst the RIAF models is LMT-Chile, although baselines between the continental United States and either the LMT or Chile are also promising for constraining RIAF parameter space. An effort should be made to include at least one of these telescopes in future observing arrays.

4. Predicted flux densities on the SMTO-LMT and CARMA-LMT baselines are well in excess of 1 Jy. The LMT should be included in a $\lambda = 1.3$ mm observing array as soon as possible, even if the surface is incomplete or not adjusted for maximum accuracy. Likewise, since many RIAF models predict flux densities on the SMTO-Chile and CARMA-Chile baselines well in excess of 0.5 Jy, a Chilean telescope should be included as soon as is feasible. Even a single 10 m or 12 m Chilean telescope has very good chances of producing detectable fringes on baselines to continental North America. If both the LMT and Chilean telescopes are available but requisite VLBI equipment such as frequency standards can be obtained for only one of the two, the LMT should be preferred initially due to the larger correlated fluxes expected on baselines to the United States.

5. Closure amplitudes will be critical, as amplitude calibration errors impose systematic errors on measured baseline flux densities that reduce their ability to constrain RIAF model parameters. At least four telescopes should be used in an observing array in order to obtain closure amplitudes. If no fourth telescope site is available at the time of reobservation, a second antenna at the CARMA site should be included in a $\lambda = 1.3$ mm observing array.

The high-frequency VLBI program at Haystack Observatory is funded through a grant from the National Science Foundation.

REFERENCES

- Bower, G. C., Falcke, H., Wright, M. C. H., & Backer, D. C. 2005, *ApJ*, 618, L29
 Bower, G. C., Goss, W. M., Falcke, H., Backer, D. C., & Lithwick, Y. 2006, *ApJ*, 648, L127
 Broderick, A. E., Fish, V. L., Doeleman, S. S., & Loeb, A. 2008, *ApJ*, submitted
 Broderick, A. E., & Loeb, A. 2005, *MNRAS*, 363, 353
 Broderick, A. E., & Loeb, A. 2006, *MNRAS*, 367, 905
 Doeleman, S. S., et al. 2008a, *Nature*, in press

- Doeleman, S. S., Fish, V. L., Broderick, A. E., Loeb, A., & Rogers, A. E. E. 2008, ApJ, submitted, astro-ph/0809.3424
- Ghez, A. M., et al. 2008, ApJ, in press
- Krichbaum, T. P. et al. 1998, A&A, 335, L106
- Marrone, D. P., Moran, J. M., Zhao, J.-H., & Rao, R. 2007, ApJ, 654, L57
- Marrone, D. P. et al. 2008, ApJ, 682, 373
- Schödel, R., Ott, T., Genzel, R., Eckart, A., Mouawad, N., & Alexander, T. 2003, ApJ, 596, 1015
- Zhao, J.-H., Young, K. H., Herrnstein, R. M., Ho, P. T. P., Tsutsumi, T., Lo, K. Y., Goss, W. M., & Bower, G. C. 2003, ApJ, 586, L29